Journal of Microscopy, Vol. 185, Pt 3, March 1997, pp. 339–353.
Received 18 April 1996; accepted 22 November 1996

Two-photon fluorescence lifetime imaging microscopy of macrophage-mediated antigen processing

T. FRENCH,* P. T. C. SO,* D. J. WEAVER, JR,† T. COELHO-SAMPAIO,‡ E. GRATTON,* E. W. VOSS, JR† & J. CARRERO†

*Laboratory for Fluorescence Dynamics, Department of Physics, and †Department of Microbiology, University of Illinois at Urbana-Champaign, Urbana, IL 61801, U.S.A.

‡Department of Bioquimica Medica-ICB, Universidade Federal Do Rio De Janeiro, Rio De Janeiro-RJ2 1910, Brazil

Key words. Antigen processing, FITC–BSA, fluorescence lifetime imaging microscopy (FLIM), fluorescence, macrophage, two-photon.

Summary

Two-photon fluorescence lifetime imaging microscopy was used noninvasively to monitor a fluorescent antigen during macrophage-mediated endocytosis, intracellular vacuolar encapsulation, and protease-dependent processing. Fluorescein-conjugated bovine serum albumin (FITC–BSA) served as the soluble exogenous antigen. As a relatively nonfluorescent probe in the native state, the antigen was designed to reflect sequential intracellular antigen processing events through time-dependent changes in fluorescence properties. Using two-photon lifetime imaging microscopy, antigen processing events were monitored continuously for several hours. During this time, the initial fluorescein fluorescence lifetime of 0·5 ns increased to $\approx$ 3·0 ns. Control experiments using fluorescein conjugated poly-L-lysine and poly-D-lysine demonstrated that the increase in fluorescence parameters observed with FITC–BSA were due to intracellular proteolysis since addition of the inert D-isomer did not promote an increase in fluorescence lifetime or intensity. Comparisons of intravacuolar and extracellular FITC–dextran concentration suggested active localization of dextran in the vacuoles by the macrophage. In addition, the kinetics of degradation observed using two-photon microscopy were similar to results obtained on the flow cytometer, thus validating the use of flow cytometry for future studies.

Introduction

Fluorescence lifetime imaging provides a way to unite structural and functional information for a more complete understanding of cellular processes, and the application of fluorescence lifetime imaging to microscopy has provided a powerful technique for elucidating several aspects of cell physiology. For example, the sensitivity of fluorescence lifetime to the microenvironment has been used to measure pH (Sanders *et al.*, 1995a), cation (Ca^{2+}, Mg^{2+}, K^{+}) concentration (Piston *et al.*, 1994; Lakowicz *et al.*, 1994) and fluorescence resonance energy transfer (Oida *et al.*, 1993; Gadella & Jovin, 1995). Other quantities that can be measured are molecular oxygen concentration, environmental polarity and local order. Fluorescence lifetime can also be used as a contrast-enhancing mechanism. Specifically, several distinct fluorophores with different lifetimes can be imaged in one picture and the fraction of each fluorophore can be resolved within a single image element (So *et al.*, 1995; Sanders *et al.*, 1995b).

Time-resolved fluorescence microscopy has advanced greatly from the first single pixel measurements (Dix & Verkman, 1990; Keating & Wensel, 1990). These first experiments deduced important cellular information such as calcium concentration or cytoplasmic matrix viscosity at selected points inside the cell. The next step in fluorescence lifetime time-resolved microscopy was to extend the single point measurements to obtain lifetime information across the entire cell. One approach is to modify a traditional laser scanning microscope to obtain time-resolved information on a point-by-point basis. Laser scanning microscopy has been used to measure three-dimensionally resolved lifetime images with confocal detection (Buurman *et al.*, 1992; Morgan *et al.*, 1992), two-photon excitation (Piston *et al.*, 1992; So *et al.*, 1995) and time-dependent optical mixing (Dong *et al.*, 1995; Müller *et al.*, 1995).

These three-dimensional (3-D) microscopic images have been routinely produced by confocal laser scanning

Correspondence to: J. Carrero, Department of Microbiology, University of Illinois at Urbana-Champaign, 131 Burrill Hall, 407 S. Goodwin Ave., Urbana, IL 61801, U.S.A. Tel: (217) 333 0299; fax: (217) 244 6697; E-mail: e-voss1@uiuc.edu

microscopes. However, the advent of the two-photon scanning technique has provided an alternative way to obtain 3-D images with several additional advantages (Denk *et al.*, 1990; Piston *et al.*, 1992). Some of these advantages include the inherent 3-D resolution without using detection pinholes, and the improved rejection of excitation light. Two-photon excitation also has a unique advantage in that photobleaching and photodamage are localized to a submicrometre region at the focal point. In contrast, a conventional scanning confocal microscope causes photobleaching and photodamage in the entire sample. One of the most important advantages of two-photon excitation is depth discrimination. For one-photon excitation in a spatially uniform fluorescent sample, equal fluorescence intensities are contributed from each *z*-section above and below the focal plane, assuming negligible excitation attenuation. This is a consequence of the conservation of energy (Wilson & Sheppard, 1984). By contrast, in the two-photon case and for objectives with a numerical aperture of 1·25, over 80% of the total fluorescence intensity comes from a 1-μm-thick region about the focal point. Thus, 3-D images can be constructed as in confocal microscopy, but without confocal pinholes. This depth discrimination effect of two-photon excitation arises from the quadratic dependence of two-photon fluorescence intensity upon the excitation photon flux which decreases rapidly away from the focal plane (Denk *et al.*, 1990).

Spatial resolution in two-photon microscopy is comparable with one-photon methods. For excitation of the same chromophore, the two-photon resolution is roughly half the one-photon confocal resolution (Sheppard & Gu, 1990; Nakamura, 1992; Gu & Sheppard, 1995). This reduction in spatial resolution is due to the larger diffraction-limited spot of the longer wavelength two-photon excitation source (double the wavelength of the one-photon source). For a 1·25-NA objective using an excitation wavelength of 960 nm, the typical point spread function has an FWHM of 0·3 μm in the radial direction and 0·9 μm in the axial direction (So *et al.*, 1995).

We have applied this new technique of two-photon fluorescence lifetime imaging microscopy to study macrophage-mediated processing of an exogenous fluorescent antigenic probe. As a prelude to monitoring continuous kinetics and rates of processing of exogenous antigens by murine macrophage, a unique fluorescent probe was developed to be used with fluorescence microscopy and flow cytometry (Voss *et al.*, 1996; Weaver *et al.*, 1996). The probe comprised the fluorescent hapten fluorescein covalently substituted to high density on a T-cell-dependent protein (BSA) carrier (Voss, 1990). On the highly substituted BSA, fluorescein hapten was relatively nonfluorescent owing to autoquenching (Voss *et al.*, 1996). Upon unfolding of the molecule or enzymatic hydrolysis of the protein backbone, densely packed fluorescein molecules were released spatially, resulting in significant fluorescence enhancement which can be continuously monitored and quantified through fluorescence microscopy or flow cytometry. It was important to note that BSA was selected as a protein antigen to develop the fluorescent probe because it possessed the appropriate biochemical properties and its immunogenic properties have been studied (Benjamin *et al.*, 1984). Critical to development of a kinetic probe for continuous monitoring, BSA is a single-chain protein existing in the monomeric state with a molecular weight of 67 kDa containing 582 amino acids and no sugar residues. It possesses extensive secondary and tertiary structure owing to the existence of many domains which have been verified by X-ray crystallographic analyses (He & Carter, 1992). Immunologically, BSA contains both continuous (linear) and discontinuous (conformation) epitopes. Polyclonal anti-BSA antibody responses are diverse and have a characteristically high affinity reflecting multiple immunoreactive epitopes and a T-cell-dependent immune response (Benjamin *et al.*, 1984).

However, prior to elicitation of a T-cell-dependent immune response, immunogenic proteins such as BSA undergo intracellular proteolytic degradation (processing) within antigen-presenting cells to relatively small peptides prior to intravacuolar binding with MHC molecules for external membrane presentation and subsequent recognition by appropriate T-cell receptors (Germain & Margulies, 1993; Cresswell, 1994). In the endocytic pathway, antigen-presenting cells internalize exogenous antigens by phagocytosis, endocytosis or both (Hardings & Geuze, 1992). Macrophage internalize antigen using both processes. Characteristically, the endocytic pathway involves acidic vacuoles: (1) early endosomes (pH 6·0–6·5), (2) late endosomes (pH 5·0–6·0) and (3) lysosomes (pH 4·5–5·0) (Kuby, 1994). Internalized antigen moves sequentially through the vacuole cascade encountering an array of proteolytic enzymes during processing (Mego, 1984; Neefjes & Ploegh, 1992). Class II MHC molecules which are linked to processing and presentation of exogenous antigens are expressed within the endocytic pathway as receptors for binding of specific peptides within the cleft of the MHC molecule (Brown *et al.*, 1993). MHC binding of peptides derived from exogenous antigens appears to occur after removal or dissociation of the invariant chain from the MHC II molecule (Levine & Chain, 1991; Cresswell, 1994; Sadegh-Nasseri, 1994). Liganded MHC molecules are subsequently transferred to the macrophage's external membrane surface where the peptide–MHC complex is recognized by T-cell receptors of CD4 T-helper cells (Neefjes & Ploegh, 1992).

In the current study, we describe the application of two-photon fluorescence lifetime imaging and this novel fluorescence probe to investigate several aspects of intracellular antigen processing. As opposed to previous techniques

such as subcellular fractionation, two-photon fluorescence imaging made it possible to monitor these events noninvasively in viable cells, providing important kinetic information about these intracellular processes.

Materials and methods

Reagents

Bovine serum albumin (BSA) was obtained from Sigma Chemical Co. (St Louis). Fluorescein isothiocyanate (FITC, isomer I) was purchased from Molecular Probes Inc. (Eugene, OR). Poly-L-lysine (53·9 kDa) and poly-D-lysine (58·9 kDa) were obtained from Sigma Chemical Co. $(FITC)_{22}BSA$ (1·0 mg mL^{-1} stock solution in 10 mM Tris, pH 8·0, and 1 mM $CaCl_2$) was synthesized as described by Voss *et al.* (1996) and stored in 50% saturated ammonium sulphate at 4 °C. FITC–dextran (Sigma Chemical; 50·7 kDa, 0·004 mol FITC per mol glucose) had an average density of 1·2 FITC per dextran molecule.

In order to determine whether the FITC linkages with ε-amino groups were stable at conditions similar to that observed in the endocytotic pathway, $(FITC)_{22}BSA$ was dialysed for 16 h at 37 °C against 0·1 M acetate buffer pH 3·5.

To ensure that antigen degradation was not due to extracellular proteases, the medium obtained from cells ($1-2\times10^6$ in 2·0 mL media) maintained for 72 h was examined for proteolytic activity using the *in vitro* fluorometric assay (Voss, 1984). Tissue culture medium was titrated (0–30 μL) against reduced $(FITC)_{22}BSA$ (65 pg). In the course of 1 h, no increase in fluorescence was noted. In the same time frame proteinase K (Stratagene) digestion of reduced FITC–BSA resulted in nearly a 29-fold increase in fluorescence.

Anti-BSA ELISA binding assay

Polystyrene wells were coated with 50 μL of 10 mg mL^{-1} FITC–BSA (Sigma Chemical Co.) in 0·1 M PO_4, pH 8·0, for 2 h at 37 °C. Polystyrene wells were washed three times with TBS-Tween and masked overnight at 4 °C with 3% nonfat Carnation milk in 0·1 M phosphate, pH 8·0. Subsequent to appropriate washes, 50 mL of IgG from a rabbit polyclonal anti-BSA reagent at 10 mg mL^{-1} was serially diluted 1:2 and added to the wells. After incubation for 2 h at 37 °C, the wells were washed three times, and HRP-labelled goat antirabbit (Zymed) at a dilution of 1:3000 in 0·1 M phosphate, pH 8·0, was added. Following incubation for 2 h at 37 °C, enzyme activity was quantified by addition of 3,3′,5,5′-tetramethylbenzidine substrate (1-Step Turbo TMB; Pierce Chemical Company). Enzyme activity was terminated by addition of 50 mL of 2 N H_2SO_4 and optical density was determined using a Dynatech MR5000 automatic 96-well microtitre reader with a 450-nm cut-off filter.

In vitro fluorescence lifetime

Fluorescence lifetime measurements were performed using an ISS K2 multifrequency phase modulation fluorometer based on the instrument described by Gratton & Limkeman (1983) and equipped with the ISS-A2D digital card. The excitation source was an air-cooled small frame argon ion laser (Omni Chrome model 532) prism tuned to 488 nm. Emission was observed through a 520 cut-on filter (Hoya). The measured quantities, phase delay and demodulation of the emission were made relative to the Rayleigh scatter of a glycogen reference. Excitation light was modulated at 12 frequencies between 50 and 250 MHz. Data were analysed using the GLOBALS Unlimited analysis program (University of Illinois, Urbana, IL). For the pH studies 0·02 μM fluorescein was prepared at pH 12 and pH 1 with NaOH and HCl, respectively. Intermediate pH solutions were prepared with 0·02 μM fluorescein in 40 mM citric phosphate buffer.

Maintenance of macrophage cell lines

Murine macrophage cell line J774 was provided by K. W. Kelley (University of Illinois, Urbana). Cells were grown in DMEM (Dulbecco's minimal eagle media, Sigma Chemical Co.) supplemented with 10% FCS (fetal calf serum), 1% NEAA (nonessential amino acids), and gentamicin–ampicillin antibiotics

Western blot analysis of intracellular localization of FITC–BSA

J774 murine macrophages were grown to a cell number of 1×10^8 and incubated with FITC–BSA for 5 min at 37 °C. The cells were gently dislodged from the plate and centrifuged at 2000*g* for 5 min. The cell pellet was resuspended in 1 mL of medium and transferred to a sterile 2-mL cryogenic vial. The probe was added directly to the cells in the cryogenic vial at a concentration of 10 μg per 10^6 cells. The reaction was allowed to proceed for 2 min and was terminated instantaneously by freezing in liquid nitrogen. After 15 min, the vial was removed from liquid nitrogen and thawed at 37 °C.

The endosomal fraction was isolated as described in Qui *et al.* (1994) and Xu *et al.* (1995). Briefly, the cells were then centrifuged at 2000*g* for 5 min and the resulting cell pellet was resuspended in 1·5 mL of homogenization buffer, HB (10 mM Tris, 1 mM EDTA, 0·25 M sucrose, pH 7·4). The cell suspension was homogenized using 20 passes in a Dounce homogenizer. The cell homogenate was diluted in 10 mL HB and centrifuged at 900*g* for 30 min at 4 °C in a Beckman

centrifuge (Model J2-21 M, JA-20 rotor) to pellet the crude membrane fraction.

The clear post-nuclear supernatant from the first spin was centrifuged at 10 000*g* for 30 min at 4 °C in a fixed angle-head rotor (Beckman L8-70 ultracentrifuge). The pellet from this spin contained the cellular mitochondrial fraction. The supernatant was layered on 30 mL of 1·07 g mL^{-1} Percoll (Sigma) and centrifuged at 50 000*g* for 45 min at 4 °C. Endosomal fractions were collected and pooled for further analysis.

The crude membrane, mitochondrial and endosomal fractions were then resolved on SDS-PAGE. Proteins were transferred to polyvinylidine difluoride membrane (Millipore Corporation). The membrane was masked using 3% nonfat Carnation milk in 0·1 M PO_4, pH 8·0, at 4 °C overnight. Following triplicate washes in TBS-Tween, the membrane was incubated with 10 mg mL^{-1} of a rabbit polyclonal anti-BSA reagent for 2 h at room temperature. Subsequent to appropriate washes, the membrane was incubated with HRP-labelled goat antirabbit antibodies (Zymed Laboratories, Inc.) diluted 1:3000 in 0·1 M PO_4, pH 8·0, for 2 h at room temperature. The Western blot was then developed using 3,3′,4,4′-diaminobenzidine substrate (Kirkegaard and Perry Laboratories, Inc.).

Wide-field microscopy

Macrophage cells incubated with FITC–BSA for varying times at 37 °C were washed and viewed using a Nikon inverted microscope (Diaphot-TMD) with a halogen lamp light source (12 V/50 W). A photomicrographic attachment (Nikon FX-35A) for a 35-mm Microflex UFX II camera with automatic exposure was used to generate colour photographs (Kodak film, Ektachrome P160, EPH-36 with ASA 1600). Cell viability controls using trypan blue exclusion were conducted to exclude the possibility that FITC–BSA labelling occurred in dead cells.

Two-photon fluorescence microscopy

Two-photon fluorescence microscopy was performed with a laser scanning microscope that had two-photon excitation and fluorescence lifetime measurement capabilities (So *et al.*, 1995). The laser used in this microscope was a mode-locked titanium sapphire (Ti-sapphire) laser (Mira 900, Coherent Inc., Palo Alto, CA) pumped by an argon-ion laser (Innova 310, Coherent Inc.). The Ti-sapphire was set to 960 nm (equivalent to one-photon excitation of 480 nm). The intensity was attenuated with a polarizer to 10 mW at the sample. At this intensity level no cellular degradation was observed during 1 h of continuous scanning. Since two-photon excitation occurs only in a limited volume, all images are three-dimensionally resolved as in a confocal image.

An *x*–*y* scanner (Cambridge Technology, Watertown, MA) directed the laser light into the microscope. The excitation light entered the Zeiss Axiovert 35 microscope (Zeiss Inc., Thronwood, NY) via a modified epiluminescence light path. The light was reflected by the dichroic mirror to the objective. The dichroic mirror was a custom-made short-pass filter (Chroma Technology Inc., Brattleboro, VT) which maximized reflection in the infrared and transmission in the blue–green region of the spectrum. The objective used in these studies was a well-corrected Zeiss 63× Plan-Neofluar with a numerical aperture of 1·25. The objective delivered the excitation light and collected the fluorescence signal. The fluorescence signal was transmitted through the dichroic mirror and refocused on the detector. An additional barrier filter was used to further attenuate the scattered excitation light. For this purpose 3 mm of BG39 Schott glass filter (CVI Laser, Albuquerque, NM) was used. A photomultiplier tube (model R3896, Hamamatsu, Bridgewater, NJ) detected the fluorescence signal from each position. A second photomultiplier tube (model R928, Hamamatsu) monitored the laser beam to correct for frequency drift of the laser pulse train.

Lifetime was measured via the frequency domain technique of heterodyning. The laser repetition frequency (80 MHz) was appropriate to measure lifetimes from 0·5 to 5 ns. The lifetime measurement uncertainty of this instrument was ± 0·2 ns.

Images were collected at a rate of 1 frame per 28 s. Each frame contained 256 × 256 pixels and covered a field of view of 36 × 36 μm (0·14 μm pixel spacing). The images presented were the result of averaging 3–4 successive frames. In regions where fluorescence intensity was too low, the lifetime was not calculated. These regions are coloured black in the lifetime images.

The murine macrophage cell line J774 was used in the two-photon microscopic studies. Cells were placed on a coverslip and grown for 12–36 h, resulting in a density of about 100 cells mm^{-2}. They were incubated with antigen at 37 °C for the prescribed time and then loaded onto a hanging drop slide without direct washing. Only cells that appeared viable, by their morphology, were chosen for further analysis. All studies included a check for autofluorescence with a control group of cells. No significant autofluorescence was detected during the studies.

Flow cytometric fluorescence intensity analysis

Two days prior to the experiment, cells were removed from primary culture and replated at 10^6 cells mL^{-1} in a 48-well tissue culture plate. On day two, the cells were pre-incubated with 10 μg mL^{-1} of $(FITC)_{10}$BSA for the designated period of time at 37 °C. Prior to flow cytometric measurements, the cells were washed in DMEM to minimize extracellular fluorescence. Then 0·6 mL of cell suspension was added to an EPICS 752 (Coulter Corporation, Miami,

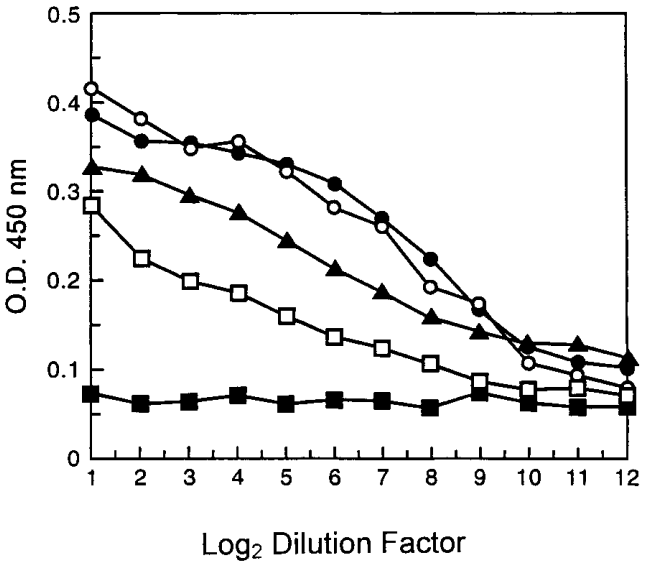

Fig. 1. Detection of BSA epitopes in $(FITC)_n$BSA probes by anti-BSA polyclonal antibodies. Polystyrene wells were coated with BSA (○), $(FITC)_3$BSA (●), $(FITC)_{10}$BSA (▲), $(FITC)_{22}$BSA (□) or milk (■), and a polyclonal anti-BSA reagent was used to detect BSA epitopes as described in the text. Binding of anti-BSA antibodies was then detected using an HRP-labelled goat antirabbit reagent.

FL) flow cytometer equipped with a CICERO data acquisition system (Cytomation, Fort Collins, CO).

Average fluorescence intensity was measured by exciting with an Innova 90-5 laser (Coherent) at 488 nm and detecting emission through a 525-nm bandpass filter. Data analysis was performed using the Cyclops software (Cytomation) and Immunobrite level III beads were used to standardize measurements.

Results

ELISA

A hyperimmune rabbit polyclonal anti-BSA reagent was used in a solid-phase ELISA to determine to what degree FITC derivatization interfered with the various BSA epitopes. Specifically, BSA, $(FITC)_3$BSA, $(FITC)_{10}$BSA and $(FITC)_{22}$BSA were absorbed to the polystyrene wells and a rabbit polyclonal anti-BSA reagent was used to detect BSA activity. Figure 1 indicates that even at the highest substitution there was significant recognition of BSA epitopes by the anti-BSA reagent. Although antibody recognition was not necessarily synonymous with MHC II recognition, the experiment provided information concerning protein epitope survival in FITC substitution reactions.

Western blot

To ensure FITC–BSA was localized to the endosomal system of the macrophage upon uptake, the cells were incubated with antigen at 37 °C for 5 min. Cells were harvested and endosomal vesicles were isolated from macrophage cell lysates. The vesicles were then analysed using both SDS-PAGE and Western blotting (Fig. 2). In both panels, lane 1 was the molecular weight standard; lane 2 was the BSA standard; lane 3 was the plasma membrane fraction; lane 4 was the mitochondrial fraction and lane 5 was the endosomal fraction. On SDS-PAGE, the stained band isolated from the vacuoles had a molecular weight consistent with BSA (≈ 67 kDa). The Western blot analysis confirmed immunologically that the band was BSA since it reacted with the polyclonal anti-BSA antibody reagent (Fig. 2B). This experiment showed that FITC–BSA was localized to the endocytotic vacuoles within 5 min but, more importantly, the probe accumulated to a greater degree within the endosomal fraction when compared with the other fractions, as evident in the intensity of the bands. These results provided further evidence that FITC–BSA was a suitable probe to monitor intracellular processing of proteins. In addition, since the probe was largely restricted to the vacuoles, the fluorescence measurements obtained using microscopy would not be affected by cytoplasmic fluorescence.

In vitro fluorescein lifetime and intensity vs. pH

In vitro fluorescein fluorescence intensity and lifetimes were measured over a pH range of 1–10 as a point of reference for the *in vivo* intensity and lifetime studies (Fig. 3). The fluorescence lifetime of fluorescein was ≈ 4 ns at a neutral or basic pH (Perrin, 1929; Bailey & Rollefson, 1953). The fluorescein fluorescence lifetime decreased to about 3·0 ns at acidic pH which corresponded to values reported for endocytic vacuoles (shaded area in Fig. 3). At pH values below 4·0, the fluorescence lifetimes decreased significantly to 0·5 ns at pH 1·0. Fluorescein fluorescence intensity as a function of pH previously measured by Martin & Lindqvist (1975) was repeated and plotted in Fig. 3. At pH 4·0 the intensity was reduced by 80% and in the far acidic range by greater than 95%.

Comparison of wide-field and two-photon microscopy

Figure 4 shows the intracellular fluorescence intensity images obtained using wide-field microscopy when soluble $(FITC)_{22}$BSA was added to macrophage cell line J774. Wide-field microscopy shows an indeterminate fluorescence from regions near the vacuoles. Images of macrophage incubated with $(FITC)_{22}$BSA using the two-photon microscope showed that the fluorescence was localized in the vacuoles. The superiority of two-photon microscopy to resolve the intracellular vacuoles of the macrophage was evident.

The 3-D resolution of the two-photon microscope proved to be crucial in distinguishing closely packed vacuoles while demonstrating that the fluorescence was localized in

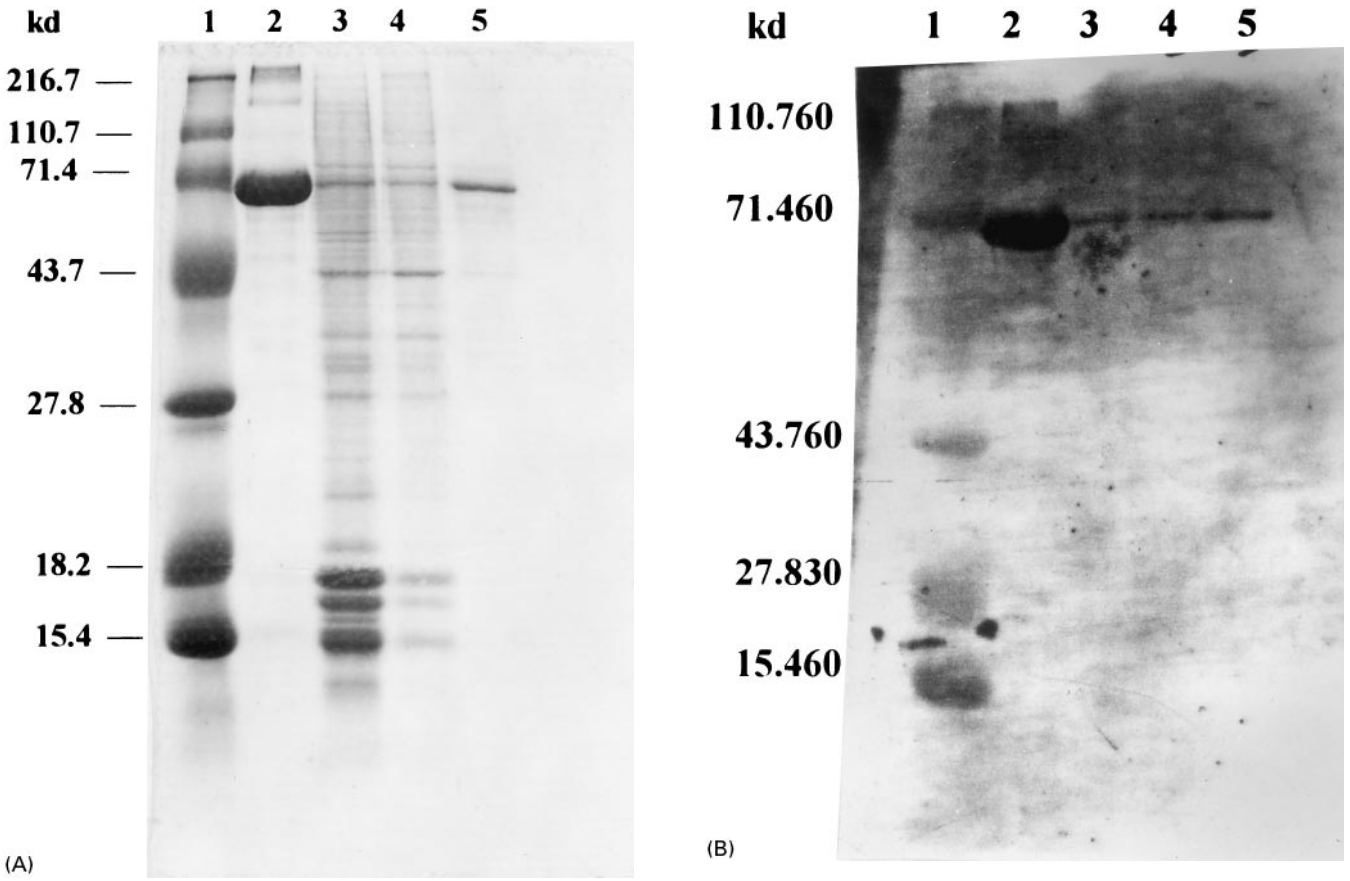

Fig. 2. Intracellular localization of FITC–BSA within murine macrophage cell line J774. Cells were incubated with antigen for 5 min and fractionated as described in the materials and methods. The fractions were resolved on SDS-PAGE (panel A) where lane 1 represents the molecular weight standards, lane 2 represents BSA, lane 3 represents the membrane fraction, lane 4 represents the mitochondrial fraction and lane 5 represents the endosomal fraction. The same fractions were also analysed by Western blotting using a polyclonal anti-BSA reagent as described in the text (panel B).

the vacuoles and not in the cytoplasm. Out-of-focus vacuoles contributed minimal fluorescence to the measured lifetime images due to the 3-D resolution. The macrophage averaged about 30 μm in length and about 10 μm in height and the endosomes were on average spherically shaped and ranged in sizes up to several micrometres in diameter. The vacuolar diameter lower limit which was reported to be 100 nm (Schwartz, 1990) was below the resolution of the microscope (0·3 μm radial, 0·9 μm axial); therefore vacuoles in that diameter range could not have been resolved.

FITC–dextran images

In vivo calibration of the FITC lifetime in acidic vacuoles was obtained with FITC–dextran. Macrophages were incubated with FITC–dextran (1 mg mL^{-1}) for 24 h and then imaged. Fluorescein fluorescence was observed only in vacuolar bodies and in the extracellular media but not in the cytoplasm (Fig. 5). The extracellular fluorescein fluorescence lifetime of FITC–dextran was 3·9 ns, corresponding to a neutral pH, and the intravacuolar lifetime was on average 3·1 ns, corresponding to an average pH of 4·0 (Fig. 3). The intravacuolar pH of 4·0 was consistent with previous reports of intravacuolar pH (Ohkuma & Poole, 1978; Tycko & Maxfield, 1982; Murphy *et al.*, 1984; Straubinger *et al.*, 1990; Aubry *et al.*, 1993). All FITC–dextran vacuoles had approximately the same fluorescence lifetime, indicating that the vacuoles were homogeneous in pH. The vacuolar fluorescence intensity was on average greater than that of the surrounding medium. In light of the quenched fluorescein fluorescence intensity expected from the low intravacuolar pH calculated from lifetime measurements, the strong intravacuolar intensity indicated that there was accumulation of FITC–dextran at high concentration in the vacuoles. The vacuolar FITC–dextran concentration was calculated to be 60 times greater than the extracellular FITC–dextran. We estimated this by multiplying the vacuolar to extracellular intensity ratio of 3 by a factor of 20, which corrected for the expected decrease in intracellular FITC intensity due to vacuolar

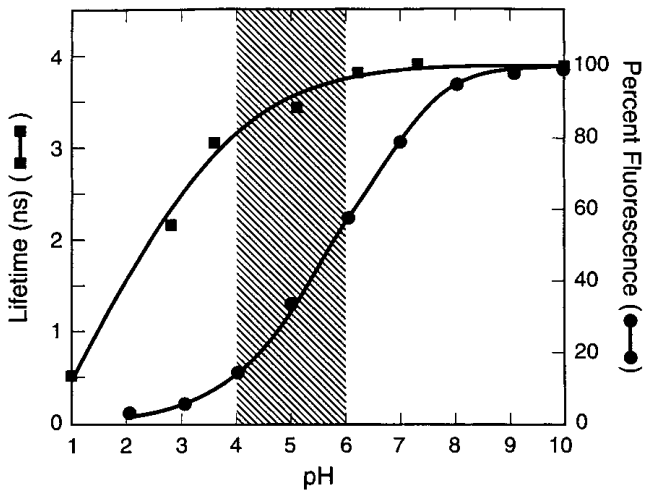

Fig. 3. Effect of pH upon the fluorescence lifetime and intensity of fluorescein. Both fluorescence lifetime (■) and intensity (●) of fluorescein at 5×10^{-9} M were measured at a pH range from 1 to 10 as described in the text.

low pH. $(FITC)_3BSA$ which lacks autoquenching due to the low FITC substitution also showed a 60-fold difference between intravacuolar and extracellular concentrations of antigen.

Synthetic peptides images

The synthetic peptides, FITC-poly-L-lysine and FITC-poly-D-lysine, provided important corroboration that fluorescein lifetime enhancement was due to proteolysis. FITC-poly-L-lysine was added to cells and incubated for 24 h (Fig. 6). The cells had bright vacuoles similar to those observed with FITC–BSA-incubated cells. Although the fluorescent lifetime of fluorescein within a single vacuole was homogeneous, there was variation between different vacuoles suggesting different stages of processing. As evident in the figure, some vacuoles had a short fluorescent lifetime (less than 0·5 ns). The intermediate lifetime ($\approx 1{\cdot}5$ ns) of some vacuoles may be attributed to two factors: (1) a

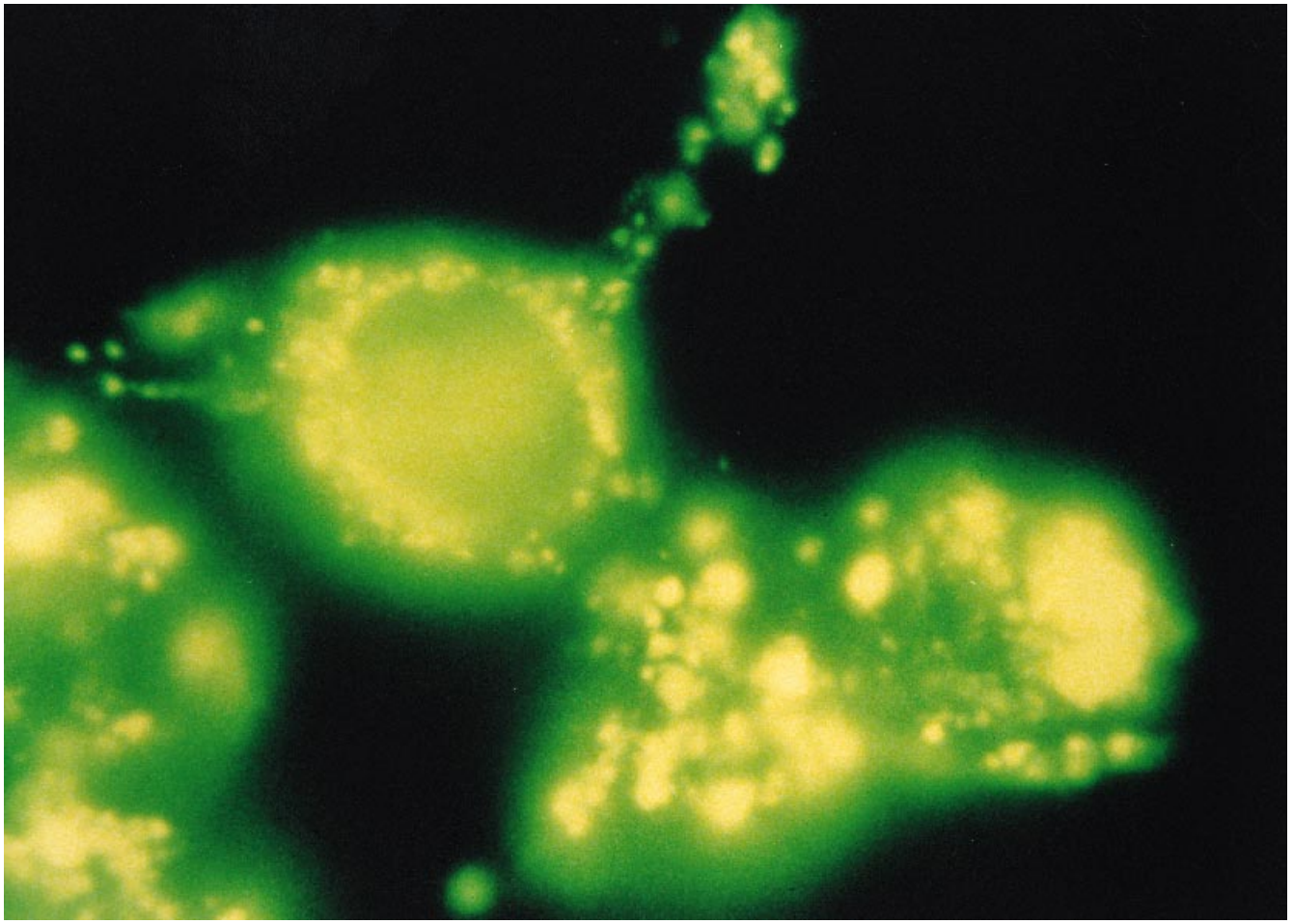

Fig. 4. Processing of $(FITC)_{22}BSA$ by murine macrophage cell line J774. Cells were incubated with $(FITC)_{22}BSA$ for 24 h, and fluorescence was monitored using wide-field fluorescence microscopy as described in the text.

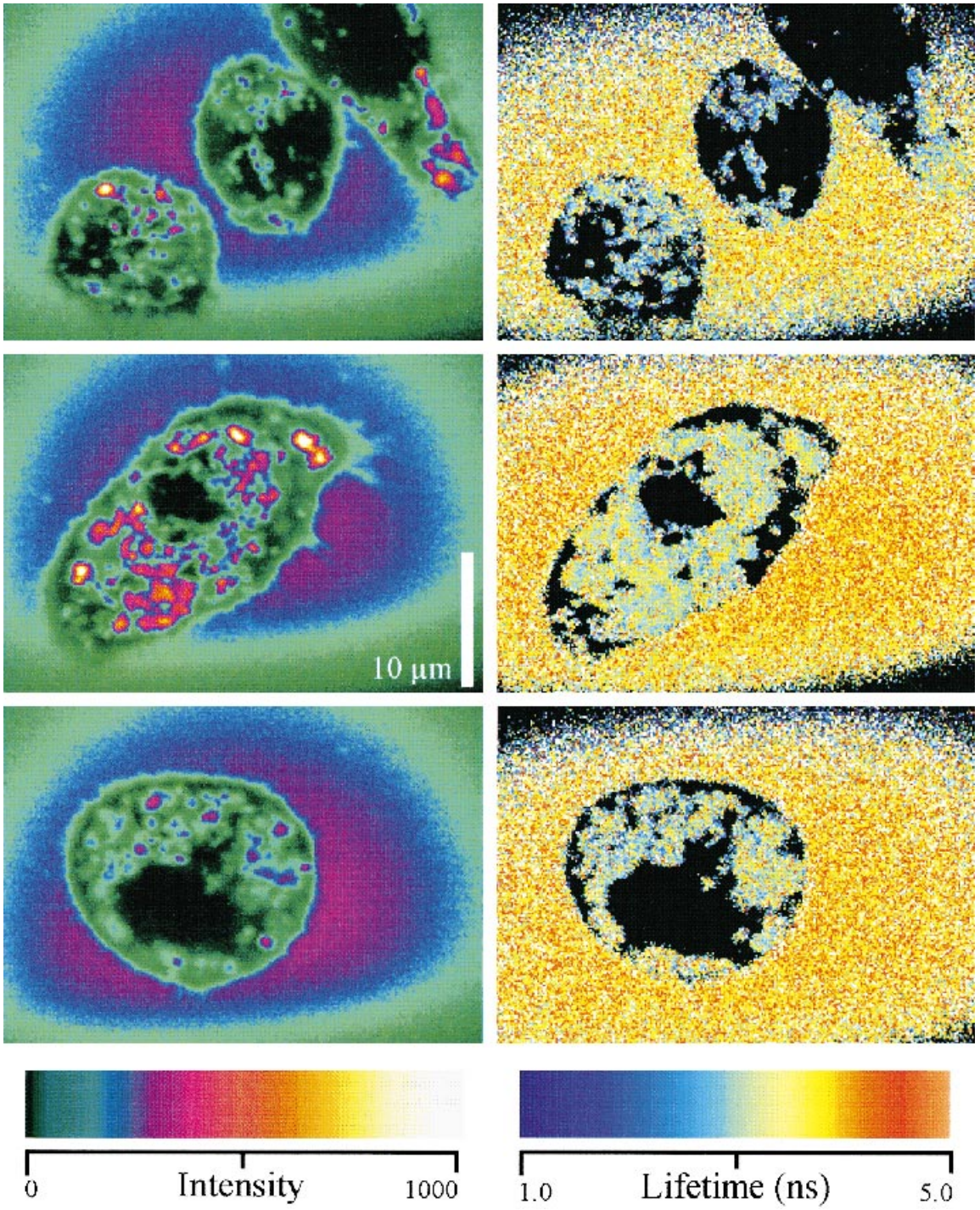

Fig. 5. Localization of FITC–dextran within macrophage cell line J774. Cells were pre-incubated with FITC–dextran and fluorescence was monitored using two-photon fluorescence microscopy. The panel on the left represents fluorescence intensity, and the panel on the right represents the fluorescence lifetime of the corresponding cell.

mixture of poly-L-lysine in various states of proteolysis or (2) low pH. The longest lifetime (≈ 4 ns) vacuoles were attributed to fully processed poly-L-lysine in a neutral pH.

The other synthetic peptide, FITC-poly-D-lysine, was used to test the hypothesis that proteolysis of FITC-poly-L-lysine produced the bright, long lifetime vacuoles. D amino acids are not susceptible to proteolytic degradation because

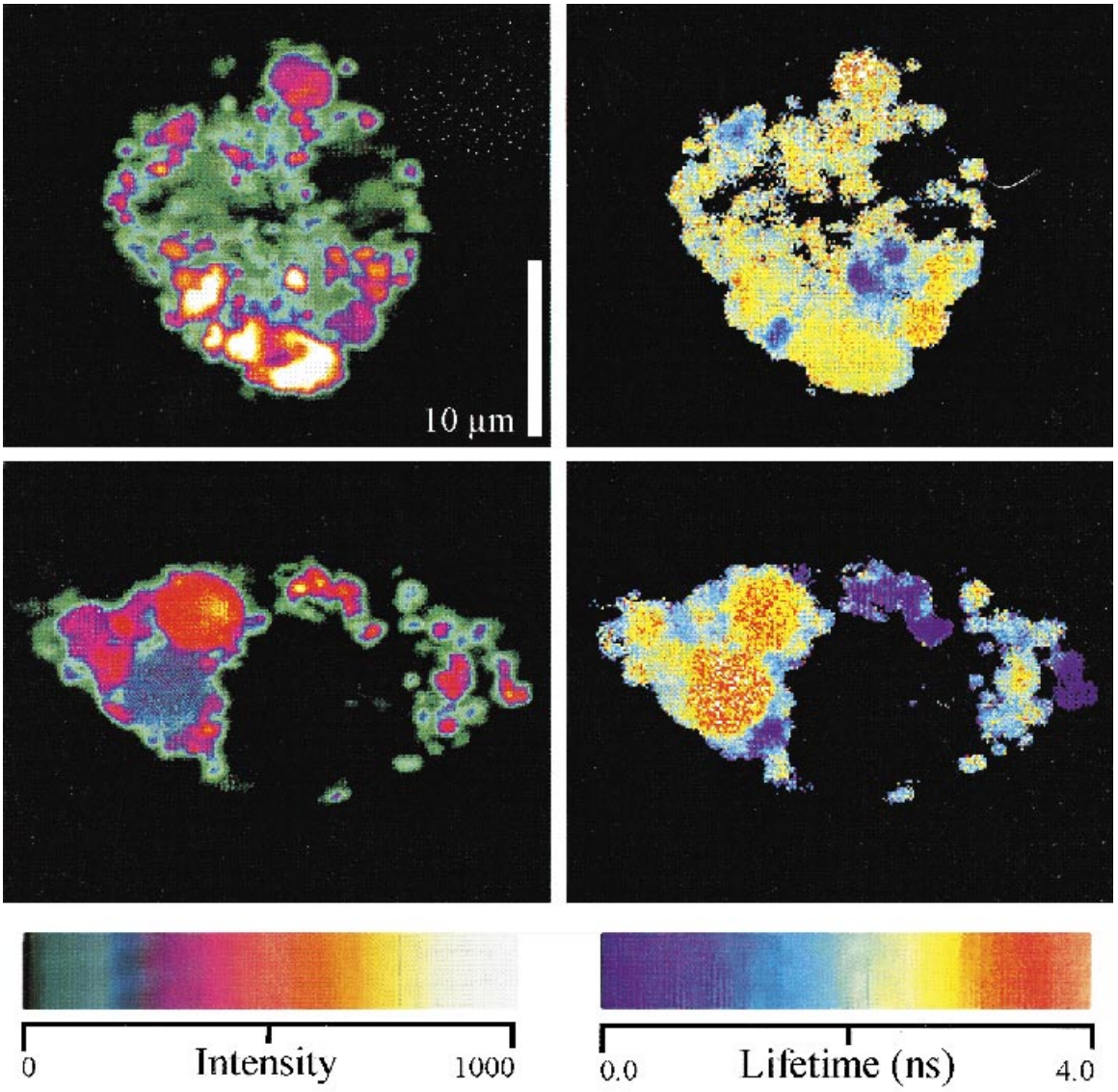

Fig. 6. Processing of FITC-poly-L-lysine by murine macrophage cell line J774. Cells were pre-incubated with FITC-poly-L-lysine, and fluorescence was monitored using two-photon fluorescence microscopy. The panel on the left represents fluorescence intensity and the panel on the right represents fluorescence lifetime.

most biological enzymes do not recognize the D configuration (Maurer, 1965; Sela, 1966; Creighton, 1993). *In vitro* incubation of various proteases from the cathepsin family of enzymes with both D- and L-FITC-conjugated polylysine showed no fluorescein fluorescence enhancement with the D isomer whereas significant enhancement was observed with the L isomer (data not shown). After incubation with poly-D-lysine for 24 h, macrophage observed using two-photon microscopy showed ingestion of the D isomer antigen as evidenced by vacuoles slightly more fluorescent than the background (Fig. 7). However, the average intravacuolar lifetime was 0·5 ns. The lack of fluorescence intensity and lifetime enhancement for FITC-poly-D-lysine corroborated the idea that the fluorescence enhancement observed with FITC-poly-L-lysine was due to proteolysis.

FITC–BSA fluorescence kinetics: two-photon microscopy

Figure 8 illustrates the effects of $(FITC)_{22}BSA$ incubation time on the measured lifetime of macrophage vacuoles. Each point was obtained by averaging the lifetimes of the vacuoles of several cells (2–15) at specific times. Representative cells from this group are presented in Fig. 9. FITC had an intrinsic lifetime of 4 ns while $(FITC)_{22}BSA$ was determined to have a lifetime of about 0·2 ns. Both the fluorescence intensity and lifetime of native $(FITC)_{22}BSA$ within the vacuoles increased as a function of incubation time with both

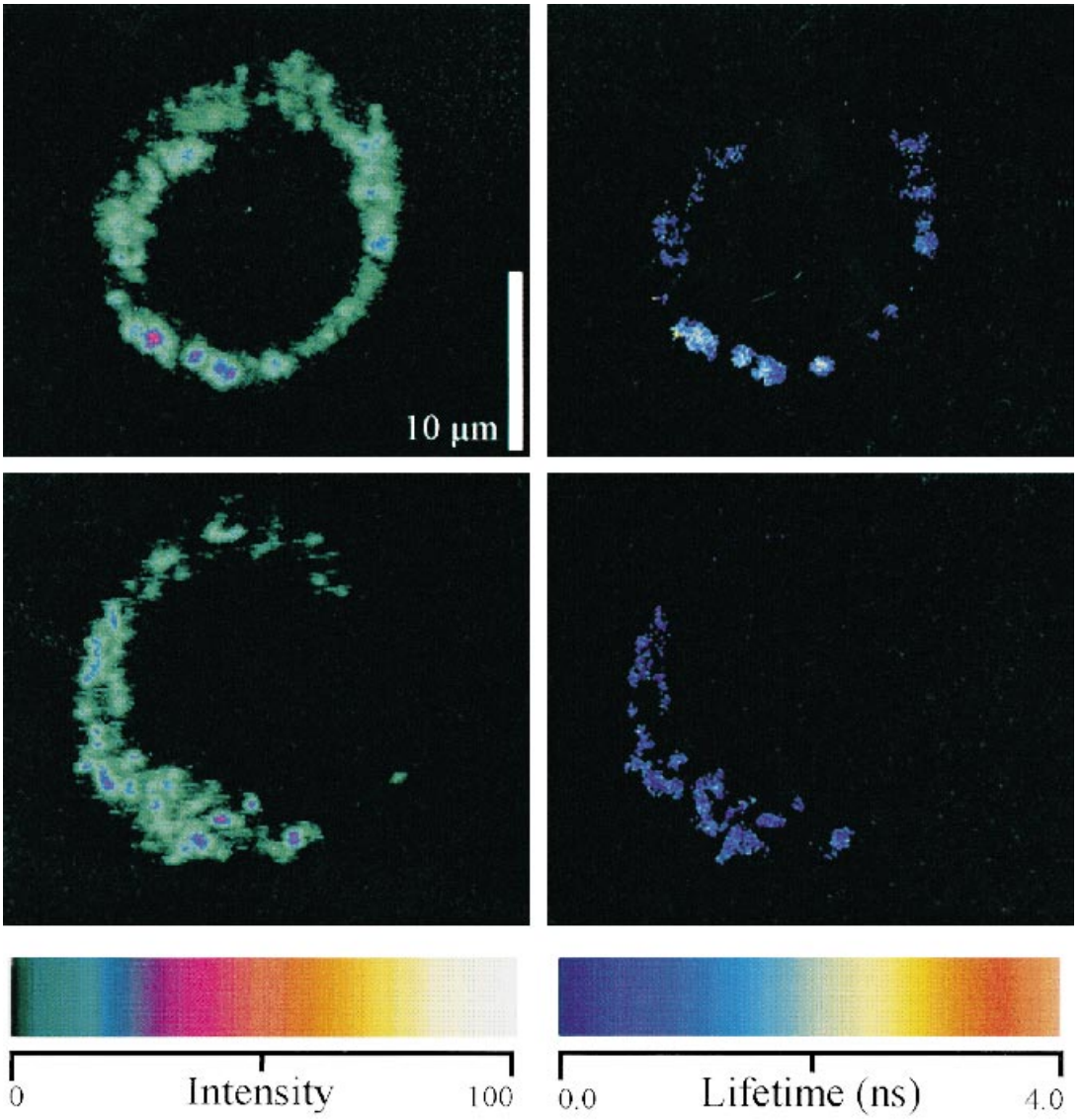

Fig. 7. Processing of FITC-poly-D-lysine by macrophage cell line J774. Cells were pre-incubated with FITC-poly-D-lysine, and fluorescence was monitored using two-photon fluorescence microscopy. The panel on the left represents fluorescence intensity and the panel on the right represents fluorescence lifetime.

fluorescence intensity and lifetime following the same kinetics, within error.

FITC–BSA fluorescence kinetics: flow cytometry

Flow cytometry can also be used to measure the time course of intracellular fluorescence intensity by measuring the total fluorescence intensity per cell. The statistics of flow cytometry have an advantage over two-photon microscopy because several thousands of cells can be monitored per minute whereas two-photon microscopy can only measure a few at a time. A comparison of the fluorescein fluorescence intensity enhancement kinetics obtained with two-photon microscopy and flow cytometry shows the kinetics were identical, within error (Fig. 8). At the very long time points the two-photon intensity deviates from the flow cytometry intensity but this may be due to the statistical advantage of flow cytometry as gauged from the two-photon error bars.

Discussion

Although the current literature describing the endocytotic pathway explains important general aspects of exogenous antigen processing-presentation events, certain specific questions remain. First, real-time kinetics of antigen uptake

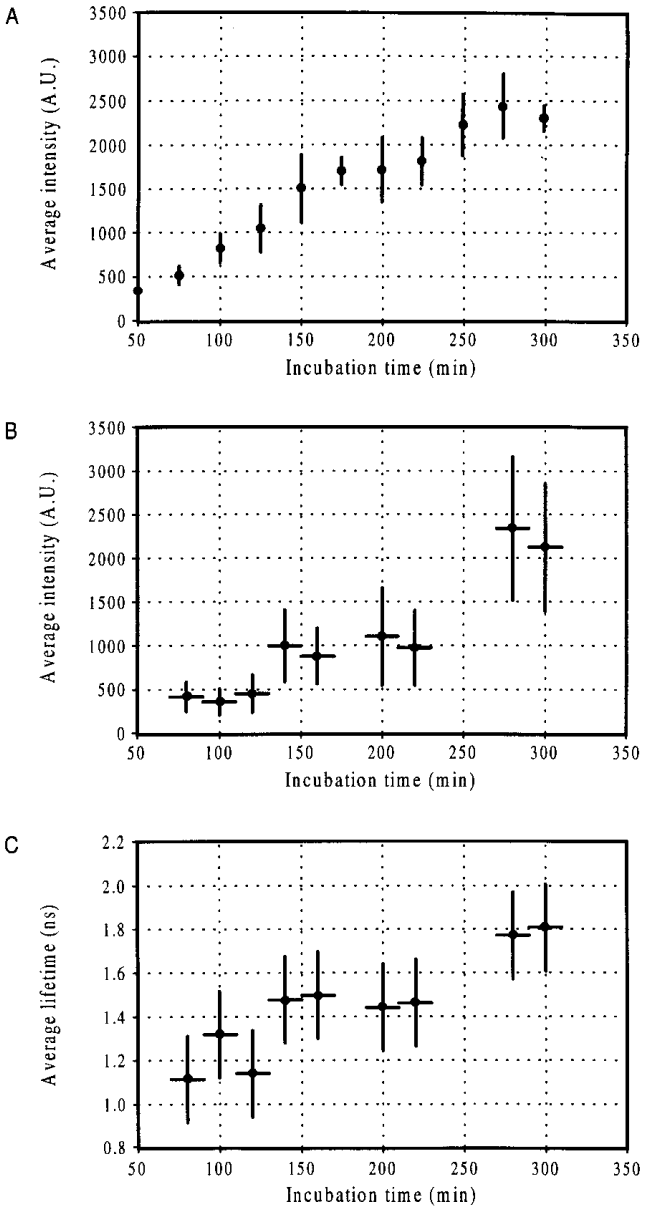

Fig. 8. Time-dependent kinetics of intracellular processing of FITC–BSA by murine macrophage cell line J774. (A) Flow cytometric analysis of fluorescence intensity. Macrophage were incubated with FITC–BSA for various periods of time, and fluorescence intensity was monitored using flow cytometry. Each point represents the average fluorescence intensity of 8000 cells, and the error bars represent the standard deviation obtained from triplicate experiments. (B) Two-photon fluorescence microscopy analysis of fluorescence intensity. The fluorescence intensity of macrophage incubated for various periods of time with FITC–BSA was monitored using two-photon microscopy. Each point was the average of 3–15 different cells. For the two-photon measurements the x error bar represents the timing variation amongst the sampled cells. The y error bar represents the instrumental standard lifetime error of 0·3 ns. (C) Two-photon fluorescence microscopy analysis of fluorescence lifetime. These measurements represent the corresponding fluorescence lifetimes of cells from panel B.

and processing have not been accurately and continuously monitored using noninvasive cellular procedures. Elucidation of the endocytotic pathway has primarily involved invasive experimental procedures, such as thin sectioning of fixed cells for electron microscopy or subcellular fractionation procedures to trace radiolabelled antigens (Qui *et al.*, 1994; Green *et al.*, 1995). Second, steps and mechanisms, such as proteolysis, involved in peptide processing and transferring to various endocytic compartments remain only partially defined (Marks *et al.*, 1990; Jensen, 1993; Xu *et al.*, 1995). Different evidence suggests that protein degradation occurs either in early endosomes or after fusion of endosomes with lysosomes (Diment & Stahl, 1985; Diment *et al.*, 1989; Collins *et al.*, 1991; Hardings *et al.*, 1991). Third, specific details of proteolytic digestion within the endocytotic pathway have not been elucidated (Puri & Factorovich, 1988; Takahashi *et al.*, 1989; Diment, 1990). For example, it has not been ascertained if proteolysis is a programmed sequential protease cascade or a relatively random degradative process.

We have applied the two-photon fluorescence lifetime technique to investigate these questions without the difficulties associated with other techniques. For example, flow cytometry has been used in previous work to study antigen processing *in vivo* (Weaver *et al.*, 1996, 1997). Although flow cytometry can quantify fluorescence intensity accurately using a large ($\approx 10^6$) sample of cells, this technique detects all cell-associated fluorescence and does not have the capability to localize the fluorescence to specific regions within the cell. To complement flow cytometry, subcellular fractionation was also used to localize the antigen to the endosome, lysosome or cell membrane, but the cells were no longer viable, rendering kinetic measurements impractical (Weaver *et al.*, 1996). Finally, electron microscopy could also be used in our studies, but the procedures required to obtain suitable electron micrographs are time consuming when compared with two-photon microscopy. In short, two-photon fluorescence lifetime microscopy was chosen as the optimal method to monitor antigen processing in macrophage because of its inherent 3-D imaging capability which made it possible to localize the fluorescent probe to specific regions within the cell. Also, since the cells were viable throughout the procedure, two-photon allowed for kinetic measurements of these processing events.

In this study, multiple lines of evidence supported the interpretation that the increases in both fluorescence intensity and lifetime of FITC–BSA observed in macrophage reflected the processing of this antigen within the endocytotic pathway. First, it was shown that the 3-D conformation of BSA was not changed significantly upon FITC substitution, indicating that the antigenic determinants of BSA were preserved, but, more importantly, a control experiment demonstrated that the thiocarbamyl linkage

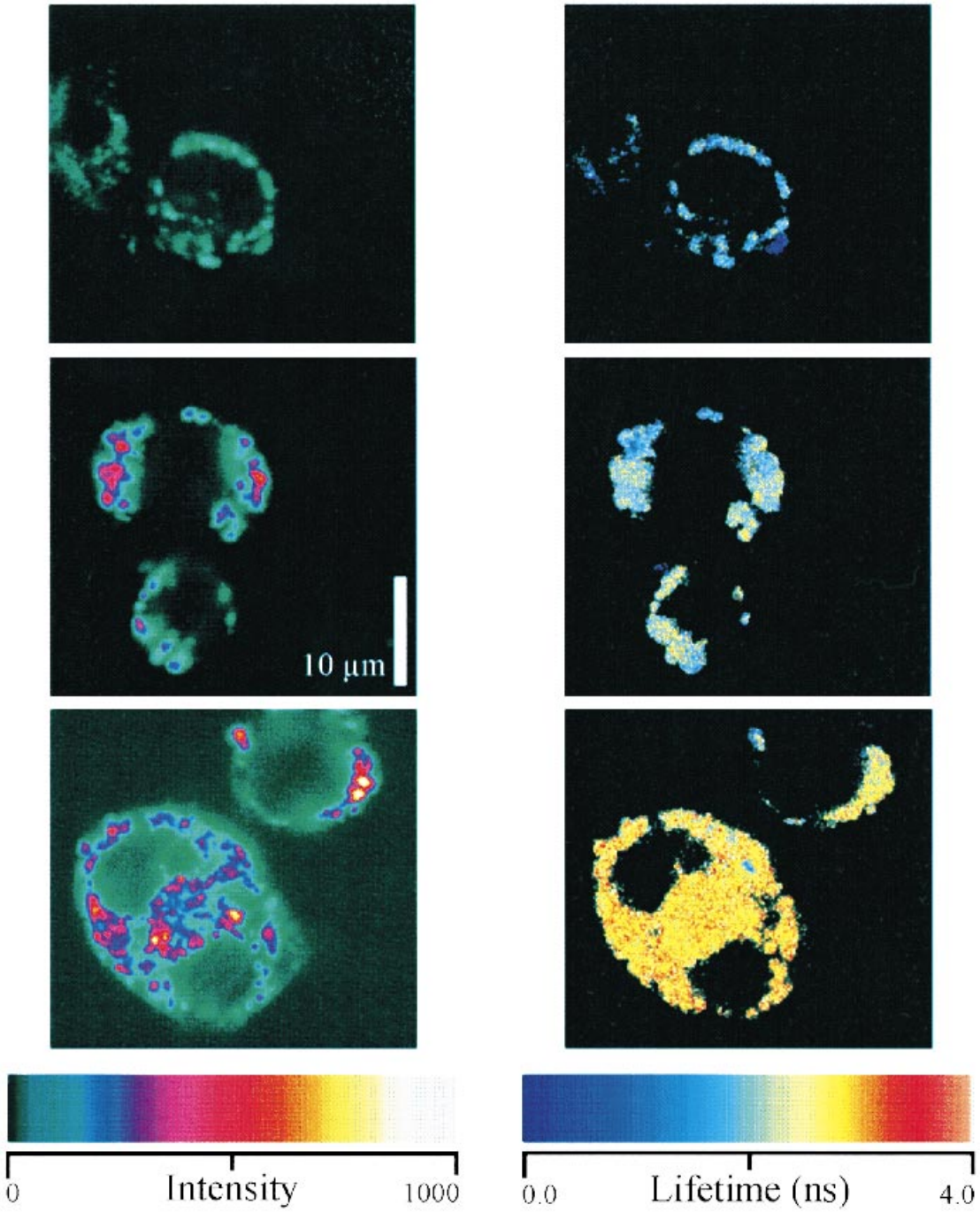

Fig. 9. Representative images of macrophage incubated with FITC–BSA for various periods. Cells were incubated with FITC–BSA and fluorescence was monitored using two-photon fluorescence microscopy. The top panel represents cells incubated for 1 h, the middle panel represents cells incubated for 5 h and the bottom panel represents cells incubated for 24 h.

between FITC and the ε amine of the lysyl residues was stable at conditions consistent with the endocytic pathway (Fig. 1). Second, when the contents of vacuoles harvested from cell lysates were analysed with SDS and Western blot, FITC–BSA was present (Fig. 2). Third, the intracellular fluorescence patterns observed with both conventional wide-field and two-photon fluorescence microscopy upon the long time incubation of macrophage with FITC–BSA showed intracellular uptake of antigen (Figs. 4 and 9). Finally, the 3-D resolution of the two-photon microscope showed conclusively that the antigen was localized in intracellular vesicles that were generally about

1 μm in diameter, which corresponded to a volume of 5×10^{-13} cm^3.

Using conventional microscopy with a photographic camera, an indeterminate fluorescence from regions near the vacuoles was observed. Such undetermined fluorescence could originate from out-of-focus vacuoles or from diffused fluorescence associated with the cytoplasm or plasma membrane (Fig. 4). The 3-D resolution of the two-photon microscope helped to verify that the cytoplasm was devoid of fluorescence. Thus, diffused fluorescence observed on conventional microscopy was due to out-of-focus vacuoles or to membrane-associated fluorescence. The latter possibility would have an important biological significance since the final destiny of antigenic peptides is presentation on cell membrane for recognition by T-cell receptor.

Also observed with conventional wide-field microscopy were bright vacuoles in macrophage that had been incubated with FITC–BSA for relatively long periods (Fig. 4). Generation of bright vacuoles from the soluble hapten–protein antigen was attributed to an active process because it required cell viability, was energy-dependent and was sensitive to a protein synthesis inhibitor (unpublished results). The brightness of the vacuoles was puzzling because fluorescein fluorescence intensity should have been strongly quenched at the low pH microenvironment known to exist in vacuoles (Fig. 3). Two possible explanations for the bright vacuoles were FITC–BSA processing resulting in extremely high localized concentrations of the antigen or an intracellular pH environment much higher than that commonly reported. Two-photon fluorescence lifetime images of FITC in macrophage vacuoles which were independent of the probe concentration separated the two possibilities. Two characteristics of FITC–dextran allowed it to be used for the measurement of intravacuolar pH: (1) it was not degraded in the endosomes and (2) the FITC:dextran ratio was 1·2:1 which prevented FITC autoquenching (Ohkuma & Poole, 1978). Therefore, the only influence on FITC lifetime would arise from the microenvironmental pH. The intravacuolar fluorescein lifetime of 3·1 ns measured in different vacuoles using the 3-D and lifetime capabilities of the two-photon microscope indicated an average pH of 4·0, consistent with pH values commonly reported. Note how the lifetime images show definitively that all the regions in the cells have the same lifetime, indicating the same pH state. The intravacuolar pH of 4·0 indicates that strong intensities with FITC–BSA were from high localized concentrations of antigen. Utilizing intensity differences, the dextran concentration was found to be 60 times greater within the vacuoles than in the extracellular medium. This was corroborated with $(FITC)_3$BSA and suggests that the uptake of immunogens by macrophage may be receptor mediated.

When using two-photon microscopy with fluorescein antigenic probes both the fluorescence intensity and the lifetime of the vacuoles were observed to increase as a function of time (Fig. 8). These two observations were consistent with the processing of the FITC–BSA. Because of the sensitivity of the antigenic probe to proteolysis, it was believed that proteolysis was the major contributor to the brightness and the long lifetimes of the vacuoles. Although different vacuoles imaged with FITC–BSA had varying lifetimes, it appeared that the lifetime within a single vacuole was homogeneous. The difference in lifetime observed amongst vacuoles was reduced with longer incubation times. The average vacuolar lifetime after 24 h of $(FITC)_{22}$BSA incubation was only 2·2 ns, which was less than the 3·1 ns obtained with the FITC–dextran. The difference in vacuolar lifetimes observed between FITC–dextran and FITC–BSA after 24-h incubations had several possible interpretations: (1) the BSA was not completely digested even after 24 h or (2) the FITC-conjugated BSA fragments were bound by an intravacuolar agent (i.e. MHC) in such a way as to quench the FITC fluorescence. Further studies using two-photon microscopy would be needed to differentiate between the two hypotheses.

Synthetic FITC-peptide conjugates (poly-L-lysine and poly-D-lysine) with the same molecular weights as BSA and significantly autoquenched in their uncleaved state were used as control reagents to test the hypothesis that the time-dependent increases in fluorescence intensity and lifetime observed with FITC–BSA were due to proteolytic degradation of the antigen. Poly-D-lysine was known to be biologically inactive and an increase in fluorescence was not expected owing to the specificity of most biological enzymes (Maurer, 1965; Sela, 1966). On the other hand, poly-L-lysine was expected to show fluorescein fluorescence enhancement because the amino acids in the L configuration would be enzymatically cleaved and fluorescence intensity and lifetime enhancement similar to FITC–BSA would ensue from relieved fluorescein autoquenching. Indeed, lifetime and intensity enhancements were observed for poly-L-lysine and not with poly-D-lysine, corroborating the idea that the time-dependent fluorescence enhancement was due to proteolysis. Moreover, the average lifetime of 4·0 ns for the macrophage poly-L-lysine vacuoles, which corresponded to neutral pH (Fig. 3), was probably due to the release of free amine, a by-product of poly-L-lysine digestion, into the vacuoles that neutralized the vacuolar microenvironment. Since the individual contributions of proteolysis, disulphide bond reduction and unfolding cannot be resolved, the kinetics in Fig. 8 were attributed to overall processing. However, the greater sensitivity of the FITC–BSA probe to proteolysis as compared with thiol reduction or unfolding (Voss *et al.*, 1996) in conjunction with these synthetic conjugate control experiments gave credence to the hypothesis that proteolysis was the main contributor to the $(FITC)_{22}$BSA lifetime increase.

FITC–BSA was used in flow cytometric kinetic studies based on the premise that time-dependent generation of fluorescence correlated with progressive processing of the FITC–BSA conjugate. Flow cytometric kinetic studies showed, in agreement with the Western blot analysis, that antigen uptake and processing occurred within 5 min and that the intensity kinetics did not change significantly with differences in antigen concentration although the level of fluorescence was affected (Weaver *et al.*, 1996). Comparison of the kinetics obtained with two-photon microscopy with those obtained with flow cytometry were identical, within error (Fig. 8). This was an important result because it was shown conclusively that fluorescein fluorescence enhancement kinetics obtained with two-photon microscopy were due to intravacuolar antigen processing and that flow cytometry can be used to monitor intravacuolar FITC–BSA processing.

Acknowledgments

We wish to express our sincerest gratitude to Gary Durack and Karen Magin of the Flow Cytometry Laboratory at The University of Illinois for their able assistance and valuable suggestions and also to Beniamino F. Barbieri at ISS (Urbana, IL) for the use of his fluorescence instrumentation.

References

Aubry, L., Klein, G., Martiel., J.-L. & Satre, M. (1993) Kinetics of endosomal pH evolution in *Dictyostelium discoideum* amoebae. *J. Cell. Sci.* **105,** 861–866.

Bailey, E.A. & Rollefson, G.K. (1953) Determination of fluorescence lifetimes of dissolved substances by a phase shift method. *J.Chem. Phys.* **21,** 1315–1322.

Benjamin, D.C., Berzofsky, J.A., East, I.J., Gurd, F.R.N., Hannum, C., Leach, S.J., Margoliash, E., Michae, J.G., Miller, A., Prager, E.M., Reichlin, M., Sercarz, E.E., Smith-Gill, S.J., Todd, P.E. & Wilson, A.C. (1984) The antigenic structure of proteins: a reappraisal. *Ann. Rev. Immunol.* **2,** 67–101.

Brown, J.H., Jardetzky, T.S., Gorga, J.C., Stern, L.J., Urban, R.G., Strominger, J.L. & Wiley, D.C. (1993) Three-dimensional structure of the human Class II histocompatibility antigen HLA-DR1. *Nature*, **364,** 33–39.

Buurman, E.P., Sanders, R., Draaijer, A., Gerritsen, H.C., van, Veen, J.J.F., Houpt, P.M. & Levine, Y.K. (1992) Fluorescence lifetime imaging using a confocal laser scanning microscope. *Scanning*, **14,** 155–159.

Collins, D.S., Unanue, E.R. & Harding, C.V. (1991) Reduction of disulfide bonds within lysosomes is a key step in antigen processing. *J. Immunol.* **147,** 4054–4059.

Cresswell, P. (1994) Assembly, transport, and function of MHC Class II molecules. *Ann. Rev. Immunol.* **12,** 259–293.

Creighton, T.E. (1993) *Proteins: Structures and Molecular Properties*. W.H. Freeman and Company, New York.

Denk, W., Strickler, J.H. & Webb, W.W. (1990) Two-photon laser scanning fluorescence microscopy. *Science*, **24,** 73–76.

Diment, S. (1990) Different roles for thiol and aspartyl protease in antigen presentation of ovalbumin. *J. Immunol.* **142,** 2221–2229.

Diment, S., Martin, K.J. & Stahl, P.D. (1989) Cleavage of parathyroid hormone in macrophage endosomes illustrates a novel pathway for intracellular processing of proteins. *J. Biol. Chem.* **264,** 13403–13406.

Diment, S. & Stahl, P. (1985) Macrophage endosomes contain proteases which degrade endocytosed protein ligands. *J. Biol. Chem.* **260,** 15311–15317.

Dix, J.A. & Verkman, A.S. (1990) Pyrene excimer mapping in cultured fibroblasts by ratio imaging and time-resolved microscopy. *Biochemistry*, **29,** 1949–1953.

Dong, C.Y., So, P.T.C., French, T. & Gratton, E. (1995) Fluorescence lifetime imaging by asynchronous pump-probe microscopy. *Biophys. J.* **69,** 2234–2242.

Gadella, T.W.J. Jr & Jovin, T.M. (1995) Oligomerization of epidermal growth factor receptors on A431 cells studied by time-resolved fluorescence imaging microscopy. A stereochemical model for tyrosine kinase receptor activation. *J. Cell Biol.* **129,** 1543–1548.

Germain, R.N. & Margulies, D.H. (1993) The biochemistry and cell biology of antigen processing and presentation. *Ann. Rev. Immunol.* **11,** 403–450.

Gratton, E. & Limkeman, M. (1983) A continuously variable frequency cross correlation phase fluorometer with picosecond resolution. *Biophys. J.* **44,** 315–324.

Green, J.M., Demars, R., Xu, X. & Peirce, S.K. (1995) The intracellular transport of MHC II molecules in the absence of HLA-DM. *J. Immunol.* **155,** 3759–3768.

Gu, M. & Sheppard, C.J.R. (1995) Comparison of three-dimensional imaging properties between two-photon and single-photon fluorescence microscopy. *J. Microsc.* **177,** 128–137.

Hardings, C.V., Collins, D.S., Slot, J.W., Geuze, H.J. & Unanue, E.R. (1991) Liposome-encapsulated antigens are processed in lysosomes, recycled and presented to T cells. *Cell*, **64,** 393–401.

Hardings, C.V. & Geuze, H.J. (1992) Class II MHC molecules are present in macrophage liposomes and phagoliposomes that function in the phagocytic processing of *Listeria monocytogenes* for presentation to T cells. *J. Cell Biol.* **119,** 531–542.

He, X.-M. & Carter, D.C. (1992) Atomic structure and chemistry of human serum albumin. *Nature*, **358,** 209–215.

Jensen, P. (1993) Acidification and disulfide bond reduction can be sufficient to allow intact proteins to bind to class II. *J. Immunol.* **150,** 3347–3356.

Keating, S.M. & Wensel, T.G. (1990) Nanosecond fluorescence microscopy: emission kinetics of Fura-2 in single cells. *Biophys. J.* **59,** 186–202.

Kuby, J. (1994) *Immunology*, pp. 243–245. W. H. Freeman & Co., New York.

Lakowicz, J.R., Szmacinski, H., Lederer, W.J., Kirby, M.S., Johnson, M.L. & Nowaczyk, K. (1994) Fluorescence lifetime imaging of intracellular calcium in COS cells using QUIN–2. *Cell Calcium*, **15,** 7–27.

Levine, T.P. & Chain, B.M. (1991) The cell biology of antigen processing. *Crit. Rev. Biochem. Mol. Biol.* **26,** 439–473.

Marks, M.S., Blum, J.S. & Cresswell (1990) Invarient chain trimers are sequestered in the rough endoplasmic reticulum in the absence of association with HLA class II antigens. *J. Cell Biol.* **111,** 839–855.

Martin, M.M. & Lindqvist, L. (1975) The pH dependence of fluorescein fluorescence. *J. Luminesc.* **10,** 381–390.

Maurer, P.H. (1965) Antigenicity of polypeptides [poly alpha-amino acids]. Immunological studies with synthetic polymers containing only D- or D- and L- alpha amino acids. *J. Exp. Med.* **121,** 339.

Mego, J.L. (1984) Role of thiols, pH and cathepsin D in the lysosomal catabolism of serum albumin. *Biochem. J.* **218,** 775–783.

Morgan, C.G., Mitchell, A.C. & Murray, J.G. (1992) Prospects for confocal imaging based on nanosecond fluorescence decay time. *J. Microsc.* **165,** 49–60.

Müller, M., Ghauharali, R., Visscher, K. & Brakenhoff, G. (1995) Double pulse fluorescence lifetime imaging in confocal microscopy. *J. Microsc.* **177,** 171–179.

Murphy, R.F., Powers, S. & Cantor, C.R. (1984) Endosome pH measured in single cells by dual fluorescence flow cytometry: rapid acidification of insulin to pH 6. *J. Cell. Biol.* **98,** 1757–1762.

Nakamura, O. (1992) Three-dimensional imaging characteristics of laser scan fluorescence microscopy: Two-photon excitation vs. single-photon excitation. *Optik*, **93,** 93–42.

Neefjes, J.J. & Ploegh, H.L. (1992) Intracellular transport of MHC class II molecules. *Immunol. Today*, **13,** 179–184.

Ohkuma, S. & Poole, B. (1978) Fluorescence probe measurement of the intralysosomal pH in living cells and the perturbation of pH in various agents. *Proc. Natl. Acad. Sci. USA*, **75,** 3327–3331.

Oida, T., Sako, Y. & Kusumi, A. (1993) Fluorescence lifetime imaging microscopy (flimscopy). *Biophys. J.* **64**, 676–685.

Perrin, F. (1929) La fluorescence des solutions. *Ann. Phys.* **12,** 169–175.

Piston, D.W., Kirby, M.S., Cheng, H., Ledere, W.J. & Webb, W.W. (1994) Two photon excitation fluorescence imaging of three-dimensional calcium ion activity. *Appl. Opt.* **33,** 662–669.

Piston, D.W., Sandison, D.R. & Webb, W.W. (1992) Time-resolved fluorescence imaging and background rejection by two-photon excitation in laser scanning microscopy. *Proc. SPIE*, **1640,** 379–389.

Puri, J.P. & Factorovich, Y. (1988) Selective inhibition of antigen presentation to cloned T cells by protease inhibitors. *J. Immunol.* **141,** 3313–3317.

Qui, Y., Xu, X., Wandinger-Ness, A., Dalke, D.P. & Pierce, S.K. (1994) Separation of subcellular compartments containing distinct functional forms of MHC II. *J. Cell. Biol.* **125,** 595–605.

Sadegh-Nasseri, S. (1994) Peptide, invariant chain, or molecular aggregation preserves class II from functional inactivation. *Antigen Processing and Presentation* (ed. by R. E. Humphreys and S. K. Pierce), pp. 171–187. Academic Press, Inc. San Diego.

Sanders, R., Draaijer, A., Gerritsen, H.C., Houpt, P.M. & Levine, Y.K. (1995a) Quantitative pH imaging in cells using confocal fluorescence lifetime imaging microscopy. *Anal. Biochem.* **227,** 302–308.

Sanders, R., Draaijer, A., Gerritsen, H.C. & Levine, Y.K. (1995b) Selective imaging of multiple probes using fluorescence lifetime contrast. *Zool. Stud.* **34,** 173–174.

Schwartz, A.L. (1990) Cell biology of intracellular protein trafficking. *Ann. Rev. Immunol.* **8,** 195–229.

Sela, M. (1966) Immunological studies with synthetic polypeptides. *Adv. Immunol.* **5,** 30.

Sheppard, C.J.R. & Gu, M. (1990) Image formation in two-photon fluorescence microscopy. *Optik*, **86,** 104–106.

So, P.T.C., French, T., Yu, W.M., Berland, K.M., Dong, C.Y. & Gratton, E. (1995) Two-photon fluorescence microscopy: time-resolved and intensity imaging. *Bioimaging*, **3,** 49–63.

Straubinger, R.M., Papahadjopoulos, D. & Hong, K. (1990) Endocytosis and intracellular fate of liposomes using pyranine as a probe. *Biochemistry*, **29,** 4929–4939.

Takahashi, H., Cease, K.B. & Berzofsky, J.A. (1989) Identification of protease that process distinct epitopes on the same protein. *J. Immunol.* **142,** 2221–2229.

Tycko, B. & Maxfield, F.R. (1982) Rapid acidifcation of endocytic vesicles containing α2-macroglobulin. *Cell*, **28,** 643–655.

Voss, E.W. Jr (1984) Immunological properties of fluorescein. *Fluorescein Hapten: An Immunological Probe* (ed. by E. W. Voss Jr), pp. 3–14. CRC press, Inc., Boca Raton, FL.

Voss, E.W. Jr (1990) Anti-fluorescein antibodies as structure–function models to examine fundamental immunological and spectroscopic principles. *Commun. Mol. Cell. Biophys.* **6,** 197–221.

Voss, E.W. Jr, Workman, C.J. & Mummert, M.E. (1996) Detection of protease activity using a fluorescence-enhancement globular substrate. *BioTechniques*, **20,** 286–291.

Weaver, D.J. Jr, Cherukuri, A., Carrero, J., Coehlo-Sampaio, T., Durack, G. & Voss, E.W. Jr. (1996) Macrophage mediated processing of an exogenous fluorescent antigenic probe: time dependent elucidation of the processing pathway. *Biol. Cell.* **87,** 95–104.

Weaver, D.J. Jr, Durack, G. & Voss, E.W. Jr (1997) Analysis of the intracellular processing of proteins: application of a novel fluorescent probe and fluorescence polarization. *Cytometry*, in press.

Wilson, T. & Sheppard, C. (1984) *Theory and Practice of Scanning Optical Microscopy.* Academic Press, New York.

Xu, X., Wenxia, S., Cho, H., Qui, Y. & Peirce, S. (1995) Intracellular transport of invarient chains-MHC class II complexes to the peptide loading compartment. *J. Immunol.* **155,** 2984–2992.